ELSEVIER

Polymer 43 (2002) 4973–4977

polymer

www.elsevier.com/locate/polymer

Surface feature size of spin cast PS/PMMA blends

C. Ton-That*, A.G. Shard, R.H. Bradley

Materials Surfaces and Interfaces Group, School of Applied Sciences, The Robert Gordon University, St Andrew Street, Aberdeen AB25 1HG, UK

Received 23 January 2002; received in revised form 13 May 2002; accepted 22 May 2002

Abstract

Thin films of polystyrene (PS)/polymethylmethacrylate (PMMA) blends have been spin cast on mica from chloroform solutions. When the concentration of PMMA in the casting solution is less than that of PS a pitted morphology is formed. The average sizes of the pits are shown to increase with both the total concentration of the casting solution and the relative concentration of PMMA. The change in pit size is explained in terms of incomplete dewetting of a PMMA solution from an underlying PS solution. For a given ratio of PMMA/PS the average pit diameters appear to increase linearly with the square of the film thickness, the gradient of which is dependent on the film composition.

Keywords: Polymer blend; Dewetting; Surface enrichment

1. Introduction

A number of technologically important properties of polymeric materials are controlled by their surface chemistry and morphology. Examples of such attributes are the contact angle with liquids, biological response and frictional properties of the materials. For polymer blends, the equilibrium composition of the surface is often different from the bulk composition due to asymmetrical environment at the air–polymer interface and larger thermal molecular motions of polymer chains in the surface region [1,2]. In an equilibrium binary blend system with similar molecular weights for each component one would expect the component with lower surface free energy to be enriched at the surface. This phenomenon of surface enrichment has been reported for the blend systems of deuterated polystyrene(d-PS)/protonated PS [3,4]; polycarbonate/poly(methyl methacrylate) (PMMA) [5,6]; and poly(ethylene-*co*-propylene)/PS [7]. In many instances, for example, blend films spin cast from a volatile solvent the surface is not at equilibrium since the solvent evaporates relatively quickly and polymer chains can be immobilised in the films before attainment of a thermodynamically favourable state. The non-equilibrium surface is thought to arise predominantly due to solvent effects [8,9]. The different solubilities of polymers in the casting solvent can cause demixing of the polymers as the solvent evaporates, leading to the component of higher solubility being enriched at the film surface [8–10].

In addition to surface composition, surface morphology is an important aspect of polymer blends. The observation of surface features in spin cast films of polymer blends can often be explained in terms of dewetting of the polymer blend from the substrate, or dewetting of one of the blend components from other blend components. When a polymeric liquid film is deposited on a substrate, the condition of wettability is governed by the spreading coefficient $S = \gamma_2 - (\gamma_1 + \gamma_{12})$. In this equation, γ_1 and γ_2 are the surface tensions of the polymer film and the substrate, respectively, and γ_{12} is their interfacial tension. For $S > 0$ the situation of complete wetting occurs, while $S < 0$ corresponds to partial wetting or non-wetting. The morphology of non-wetting, destabilised films can vary from characteristic spinodal dewetting patterns to discrete cylindrical holes, as predicted from short- and long-range intermolecular interactions [11–13]. Both grains/matrix and holes/matrix morphologies have been observed on the polymeric blend films, depending on the blend compositions [14–16], film thickness [2,17] and casting solvent [9]. It has been shown that changing the relative homopolymer proportions in such blends varies the domain structure and surface morphology [16–18]. Previously, we have described the surface analysis of PS/PMMA blends spin cast from chloroform solutions [15]. The spin cast blend

* Corresponding author. Address: Department of Engineering, University of Cambridge, Cambridge CB2 1PZ, UK. Tel.: +44-1223-332608; fax: +44-1223-262662.

E-mail address: ct255@eng.cam.ac.uk (C. Ton-That).

0032-3861/01/$ - see front matter
PII: S0032-3861(02)00333-6

films were found to possess non-equilibrium surfaces with a significant excess of PMMA, which may result from the initial formation of a bilayer PMMA solution on top of a PS solution [15,19]. Characteristic surface features of the cast films are holes and islands with typical sizes ranging from tens of nanometers to several micrometers. Annealing these films above the glass transition temperatures of the polymers resulted in dewetting ($S = -4.3\ \mathrm{mJ/m^2}$) of PMMA from the PS-rich phase [19]. The purpose of this study is to investigate relationship between the surface structure and film thickness for the PS/PMMA blends.

Brochard-Wyart et al. [13,20] have presented a theoretical treatment of dewetting for a liquid (A)/liquid (B) system. The lower layer behaves like a liquid when $\eta_B < \eta_A/\theta_E$, where η_A and η_B are the viscosity of liquids A and B, and θ_E is the equilibrium contact angle of liquid A on liquid B. This condition can be easily met for the solvent-cast PS/PMMA films since θ_E is small. For a sufficiently thin (less than a few hundred nanometers), non-wetting liquid film of thickness e on a liquid substrate, the surface thermal fluctuations will be amplified due to long-range intermolecular forces. The van der Waals interaction energy per unit area between two parallel surfaces separated by a distance e is given by [21]

$$P(e) = -\frac{A}{12\pi e^2} \tag{1}$$

In this equation, A is the Hamaker constant. For a non-wetting liquid, A may be positive, the excess intermolecular forces $\Pi(e) = -\partial P(e)/\partial e$ decreases in magnitude with an increase in local film thickness, leading to pressure gradient and flow of material from thinner to thicker regions. This destabilisation process can result in a rupture of the film into holes of average size proportional to e^2/a [20]. Molecular length a is defined by $a^2 = |A|/6\pi\gamma_A$, where γ_A is the surface tension of liquid A.

2. Experimental

PS ($M_w = 280\,000$) and poly(methyl methacrylate) (PMMA) ($M_w = 350\,000$), were used as obtained (Sigma Aldrich, UK). Glass transition temperatures of the PS and PMMA, measured by differential scanning calorimetry, were 106 and 111 °C, respectively. Polymer solutions were prepared by dissolving each polymer in chloroform (concentration expressed as % w/v). Polymer blend solutions were made by mixing the homopolymer solutions in the desired proportions. Polymer films were prepared by spin casting 60 μl aliquots of the polymer solutions under ambient conditions onto a freshly cleaved mica substrate, which was rotated at ~3000 rpm for 2 min. Film thickness was evaluated by scratching through the polymer film down to the substrate using stiff AFM cantilevers and high loading force, as described previously [22].

Surface chemical compositions of the films were measured by XPS using a Kratos Axis 5-channel HSi spectrometer with monochromated Al Kα (1486.6 eV) X-rays operated at 150 W. The attenuation length of C 1s photoelectrons in PS and PMMA is approximately 3.0 nm [23]. The sample analysis chamber of the XPS instrument was maintained at a pressure of $\sim 4 \times 10^{-9}$ Torr. Charge neutralisation was used for all the samples to offset charge accumulation with standard operating conditions for insulator surfaces, −2.8 V bias voltage, −1.0 V filament voltage, and +1.9 A filament current. Elemental compositions were calculated from the areas of carbon 1s (C 1s) and oxygen 1s (O 1s) peaks in survey spectra, collected at a pass energy of 80 eV, using appropriate relative sensitivity factors. Detailed surface chemical composition was obtained by analysis of C 1s envelopes collected at a pass energy of 20 eV. Chemical shift peaks are charge referenced to the C–C/C–H peak at 285 eV. Peak analysis was carried out using Kratos software and also version 1.5 of the spectral data processor (XPS International). The peaks in the blend spectra were assigned to the chemical groups found in the PS and PMMA homopolymers [15,24], typical peak-fitted examples are shown in Fig. 1 for the single component and blended films. Binding energies for the chemical components are used as following: C–C/C–H at 285.0 eV, β-shifted carbon at 285.7 eV, methoxyl at 286.8 eV, ester at 289.1 eV and π–π^* shake-up satellites at shifts of 6–8 eV. For quantitative analysis of the surface composition for the blend, the surface PMMA molar concentration was evaluated by using either elemental O/C ratio from survey spectra or percentage of the ester group in the C 1s envelopes, as described in a previous paper [15].

Surface topography of the films was characterised by AFM under ambient conditions, using a digital instruments (DI) multimode SPM IIIa system. All imaging was performed in tapping-mode™ using silicon tips with cantilever driving amplitudes of 45–80 nm and feedback achieved at 60–80% of the driving amplitude. Multiple images of all the blend films were acquired, enabling statistical analysis of data. To quantify surface feature sizes, we analysed 10–15 typical pits randomly selected on different AFM images. Width at half depth of the surface pits was measured by cross-section analysis using commercial DI software (version 4.23r3).

3. Results and discussion

Fig. 2 demonstrates the range of typical morphologies exhibited by blend films. Both pure homopolymers produce a smooth, homogenous film that are typically free from surface features and pinholes. Blends of PS and PMMA display either a pitted surface or a granular surface. The important criterion for the production of one or the other morphologies appears to be the relative concentration of the two polymers in the casting solution. Pitted surfaces are exhibited in films spin cast from a solution containing a PS/PMMA ratio of 50% or greater. Granular surfaces result

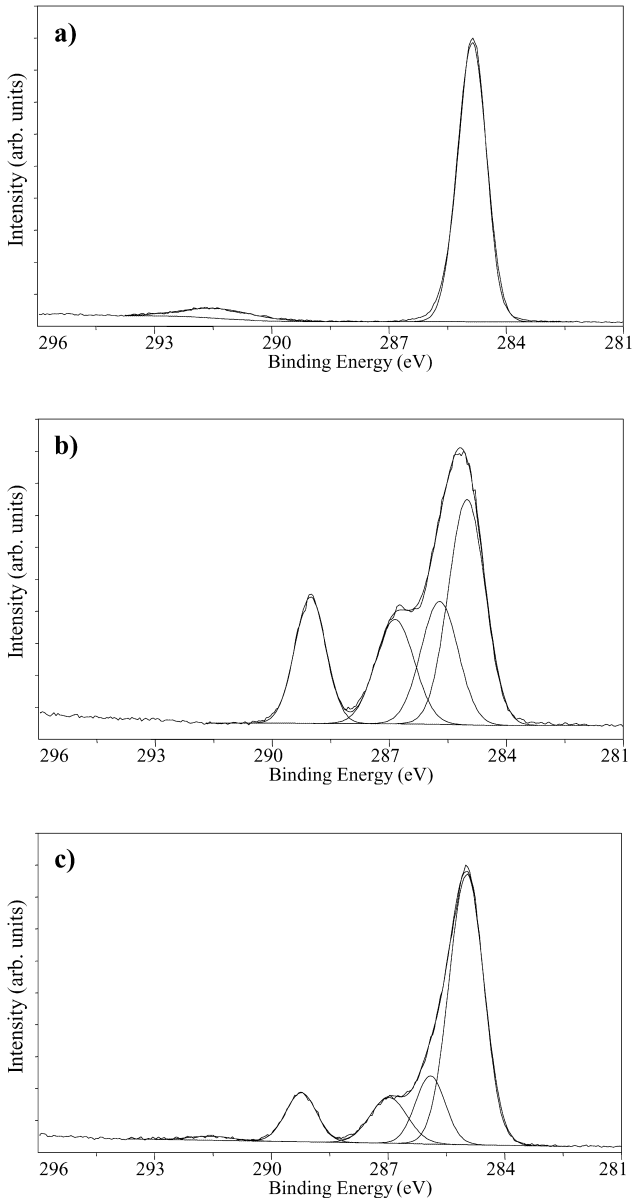

Fig. 1. High-resolution C 1s spectra with fitted curves for PS (a), PMMA (b) and 50%PS/50%PMMA blend (c) films. Film thickness was measured at 11.9 ± 2.1 nm for the blend film.

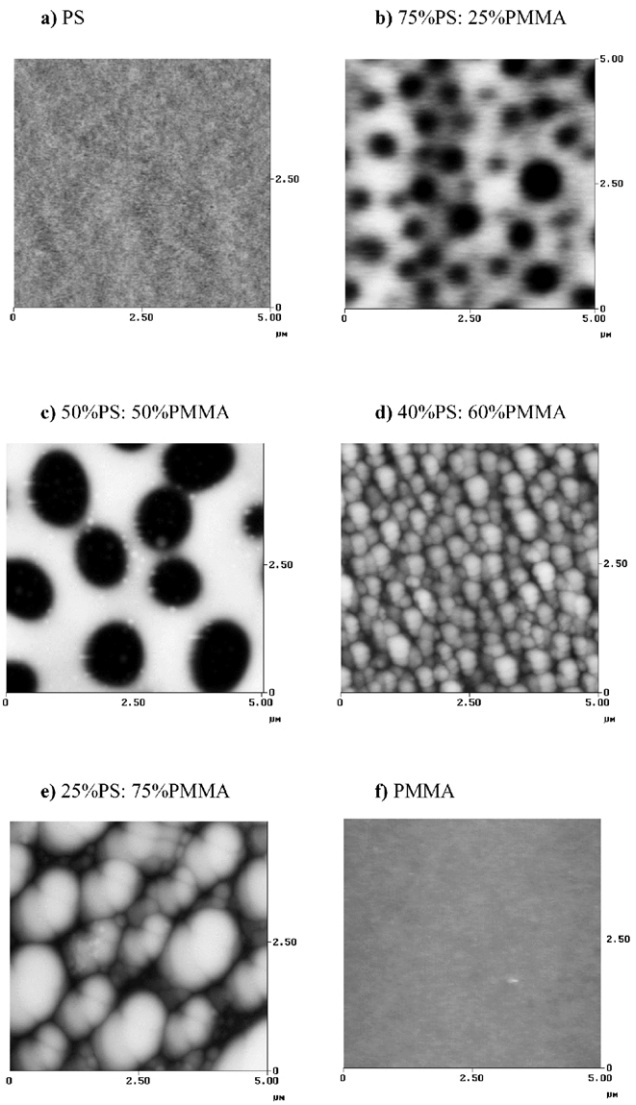

Fig. 2. AFM topographical images of PS/PMMA films with different blend compositions. The films were cast from 1% w/v solutions and the resulting film thickness was measured at 65 ± 17 nm for all the films shown. *Z* ranges of the images are: (a, f) 20 nm, (b) 120 nm, (c) 140 nm, and (d, e) 100 nm.

from spin casting a solution which has a greater concentration of PMMA than PS. All of the blend films display a large surface excess of PMMA, which indicates that these surfaces are not at thermodynamic equilibrium since the surface energy of PS is lower than that of PMMA [15,17]. The reason for the higher surface concentration of PMMA is unknown at present, but is probably related to the differing solubilities of PMMA and PS in chloroform.

Previously, we have postulated that the pitted morphology arises as a result of the formation of a phase separated bilayer of a PMMA rich solution on top of a PS rich solution in chloroform [15]. The pits form as a result of the initial stages of PMMA dewetting from the PS underlayer. This process is not completed within the timescale of solvent evaporation and hence PS is not present at the blend surface. This view appears to be supported by the subsequent annealing of the pitted films, following which the PS appears at the blend surface first expressing itself at the floor of the pits [19]. The average pit diameter increases as the film thickness increases, as shown in Figs. 3 and 4. The AFM images shown in Fig. 3 are taken from the centre of the sample; toward the edge of the mica sample the pits become somewhat elongated, presumably due to the effect of centrifugal force away from the centre of sample rotation. The pits in the imaged areas are approximately spherical in shape and appear to be evenly distributed across the surface. It can be seen that in some areas the edges of individual pits have merged, and the distorted shapes of some of the pits are probably formed from complete merger of two or more initially spherical

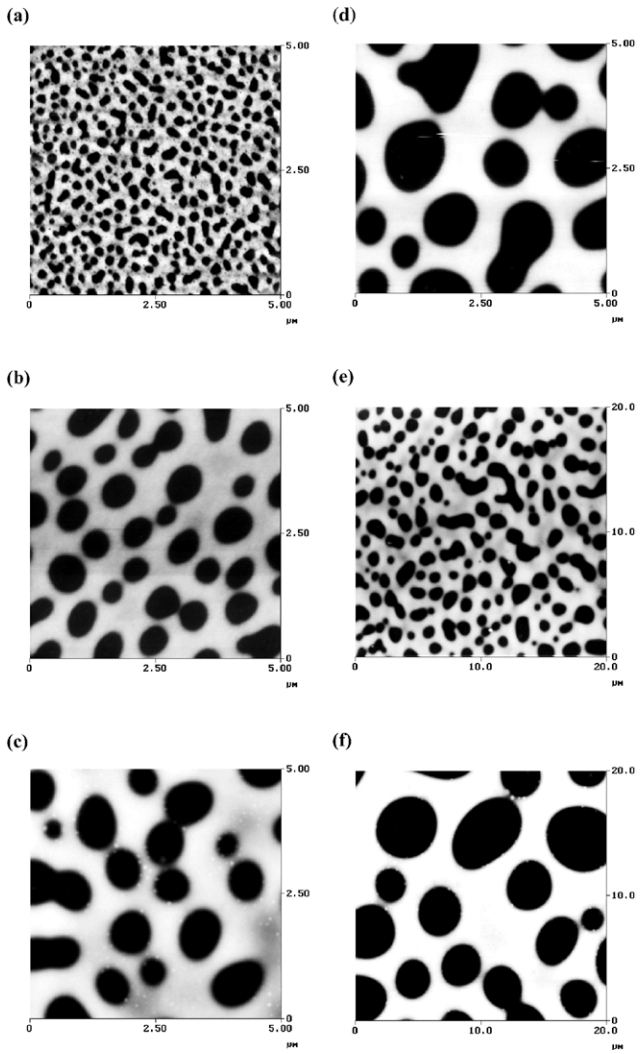

Fig. 3. AFM topographical images of 50%PS/50%PMMA blend films showing the increase in pit sizes with film thickness: (a) 13 nm thick film (z range of the image = 17 nm); (b) 25 nm (z range = 45 nm); (c) 38 nm (z range = 70 nm); (d) 63 nm (z range = 120 nm); (e) 95 nm (z range = 160 nm); and (f) 127 nm (z range = 160 nm).

pits. Although the size of the pits varies with film thickness the features appear to scale accordingly, note, for instance, the similarity in appearance of Fig. 3(a) and (e) or (d) and (f) which are displayed on different scales. Fig. 4 also displays the XPS results, in which it can be seen that the majority of these films have a large surface excess of PMMA as described previously. Films which have a thickness of a similar magnitude to the XPS sampling depth (approximately 9 nm) demonstrate the presence of PS. The XPS data in these cases are consistent with an overlayer of PMMA on PS, the PMMA thickness being approximately the product of the total film thickness and the weight fraction of PMMA in the casting solution (relative to PS). All of the blend films studied here thus have an almost pure PMMA surface.

The dewetting dynamics of a liquid layer on a liquid substrate have been described in detail [13,20] and the size of features should be proportional to the square of the top

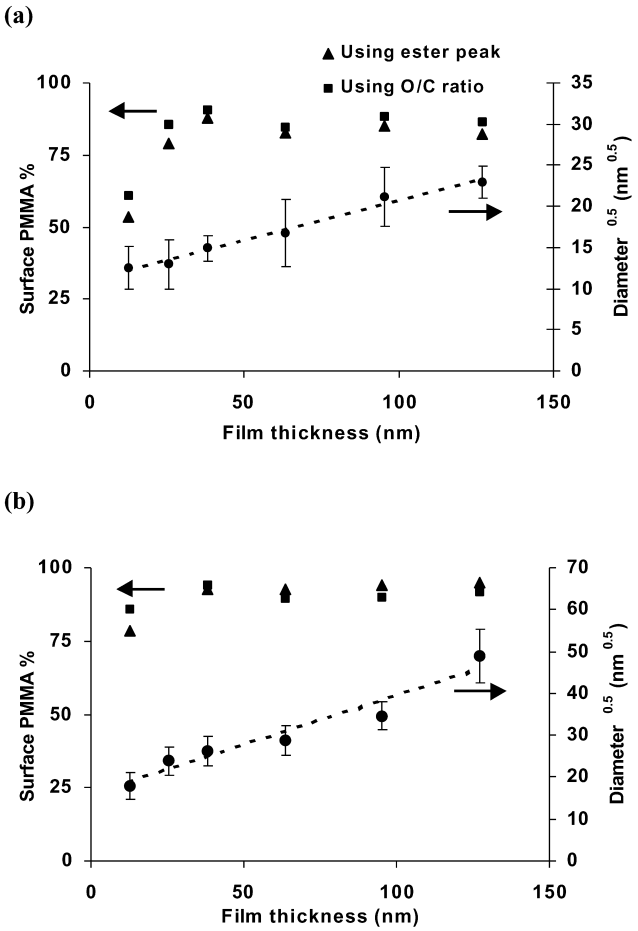

Fig. 4. Variations of averaged square root of pit diameters and PMMA surface concentrations with film thickness for blend film composition of 75%PS/25%PMMA (a) and 50%PS/50%PMMA (b). The lines are linear regression of diameter$^{0.5}$ versus thickness data. The error bars represent a range of one standard deviation.

layer film thickness, as discussed in Section 1. In the case of spin cast PS/PMMA blend films the PMMA overlayer thickness is the parameter of importance. In Fig. 4 the square root of the average pit diameter is plotted against the total film thickness for two relative blend compositions (25 and 50% PMMA, respectively). For a given blend composition the square root of the pit diameter appears to increase linearly with the film thickness. If it is assumed that the overall composition of the film is the same as the solution composition and that complete phase separation into a bilayer system has occurred then one may expect the square root of the pit diameter to be proportional to the thickness of the PMMA overlayer and also the total film thickness. Fig. 4 demonstrates that this is not the case, the linear regression to the data points does not in either case approach the origin.

The simple relationship described above cannot be used to predict the pit diameters of spin cast blends of PMMA and PS. This is hardly surprising if it is considered that, in addition to the assumptions made above one should also take into consideration the dynamics of polymer phase

separation and the rapidly changing viscosity of the polymer phases as solvent evaporation occurs. However, it is interesting to note that the gradients of the linear regressions given in Fig. 4 appear to be strongly dependent upon the film composition. For blends of 25% PMMA the gradient is 0.095 and for the 50% blend it is 0.22. Thus, the gradient appears to scale with the relative concentration of the polymer solution and a simple empirical relationship is indicated, although at this stage unobtainable without a substantially larger dataset.

These results demonstrate that for the PMMA/PS system, and possibly other polymer blend combinations [25–27], the size of features of spin cast films can be controlled by changing the concentration of the casting solution (both the total and relative concentrations of the two polymer components are important). It is possible, therefore, to create films of a desired thickness with a predictable surface feature size in a simple, one step process. Further work needs to be carried out to investigate the minimum and maximum size of features available by this technique, the effect of spin rate and solvent evaporation rate and the empirical relationship between polymer concentration and feature size. Furthermore, the ability to complete the dewetting at the floor of the pits has been demonstrated [19] and this leads to the production of distinct surface chemical features with a characteristic scale length, which may have potential technological applications, such as directed cell growth [28].

4. Conclusion

Spin cast blends of PMMA and PS in chloroform display a pitted morphology when the PMMA concentration in the casting solution is less than the PS concentration. The average size of the pitted features has been measured by AFM and found to increase as the concentration of the casting solution is increased. It is postulated that the pits are a result of an incomplete dewetting process of a bilayer system, with PMMA on top of PS. The average pit size appears to demonstrate a simple empirical relationship to the casting solution concentration although a much greater range of data is required to determine the relationship.

References

[1] Garbassi F, Morra M, Occhiello E. Polymer surfaces: from physics to technology. Chichester: Wiley; 1998. p. 49.
[2] Tanaka K, Takahara A, Kajiyama T. Macromolecules 1995;28:934–8.
[3] Jones RAL, Kramer EJ, Rafailovich MH, Sokolov J, Schwarz SA. Phys Rev Lett 1989;62:280–3.
[4] Schwarz SA, Wilkens BJ, Pudensi MAA, Rafailovich MH, Sokolov J, Zhao X, Zhao W, Zheng X, Russell TP, Jones RAL. Mol Phys 1992;76:937–50.
[5] Chiou JS, Barlow JW, Paul DR. J Polym Sci B 1987;25:1459–71.
[6] Lhoest JB, Bertrand P, Weng LT, Dewez JL. Macromolecules 1995;28:4631–7.
[7] Overney RM, Leta DP, Fetters LJ, Liu Y, Rafailovich MH, Sokolov J. J Vac Sci Technol 1996;14:1276–9.
[8] Garbassi F, Morra M, Occhiello E. Polymer surfaces: from physics to technology. Chichester: Wiley; 1998. p. 291.
[9] Walheim S, Boltau M, Mlynek J, Krausch G, Steiner U. Macromolecules 1997;30:4995–5003.
[10] Schmidt JJ, Gardella JA, Salvati L. Macromolecules 1989;22:4489.
[11] Fondecave R, Brochard-Wyart F. Macromolecules 1998;31:9305–15.
[12] Herminghaus S, Jacobs K, Mecke K, Bischof J, Fery A, Ibn-Elhaj M, Schlagowski S. Science 1999;282:916–9.
[13] Brochard-Wyart F, Martin P, Redon C. Langmuir 1993;9:3682–90.
[14] Gutmann JS, Muller-Buschbaum P, Schubert DW, Stribeck N, Stamm M. J Macromol Sci, Phys 1999;B38:563–76.
[15] Ton-That C, Shard AG, Teare DOH, Bradley RH. Polymer 2001;42:1121–9.
[16] Davies MC, Shakesheff KM, Shard AG, Domb A, Roberts CJ, Tendler SJB, Williams PM. Macromolecules 1996;29:2205–12.
[17] Tanaka K, Takahara A, Kajiyama T. Macromolecules 1996;29:3232–9.
[18] Jackson ST, Short RD. J Mater Chem 1992;2:259–60.
[19] Ton-That C, Shard AG, Daley R, Bradley RH. Macromolecules 2000;33:8453–9.
[20] Brochard-Wyart F, Daillant J. Can J Phys 1990;68:1084.
[21] Israelachvili J. Intermolecular and surface forces, 2nd ed. London: Academic Press; 1992. p. 177.
[22] Ton-That C, Shard AG, Bradley RH. Langmuir 2000;16:2281–4.
[23] Lukas J, Jezek B. Collect Czech Chem Commun 1983;48:2909–13.
[24] Beamson G, Briggs D. High resolution XPS of organic polymers. New York: Wiley; 1992.
[25] Affrossman S, O'Neill SA, Stamm M. Macromolecules 1998;31:6280–8.
[26] Muller-Buschbaum P, Gutmann JS, Stamm M. J Macromol Sci, Phys 1999;B38:577–92.
[27] Muller-Buschbaum P, Gutmann JS, Stamm M. Macromolecules 2000;33:4886–95.
[28] Dewez JL, Lhoest JB, Detrait E, Berger V, DupontGillain CC, Vincent LM, Schneider YJ, Bertrand P, Rouxhet PG. Biomaterials 1998;19:1441–5.